DISSIPATION, RADIATION, DUFOUR AND SORET EFFECTS ON HEAT AND MASS TRANSFER OF CHEMICALLY REACTING FLUID WITH HEAT GENERATION

Supported by tetfund

J. A. Gbadeyan[1], T. M. Asiru[2] and H. A. Isede[3]
[1]Department of Mathematics, University of Ilorin, Kwara State, Nigeria
[2]Department of Mathematics, Emmanuel Alayande College of Education, Oyo, Oyo State, Nigeria
[3]Department of Mathematics, University of Lagos, Akoka, Lagos State, Nigeria
*Corresponding author: afeisede@yahoo.com

Received: December 05, 2019 **Accepted:** February 24, 2020

Abstract: This study investigates the effects of dissipation, radiation, Dufor, Soret, heat and mass transfer on a laminar free convective flow of a viscous incompressible, electrically conducting chemically reacting fluid past an impulsively started moving plate adjacent to non-Darcy porous regime in the presence of heat generation. The governing equations are reduced to two-dimensional and two dependent problems involving velocity, temperature, and concentration with appropriate boundary conditions. The Rosseland diffusion approximation was used to analyze the radiative flux in the energy equation which is appropriate for non-scattering media. The governing equations for the model were simplified and nondimensionalised using dimensionless quantities. The dimensionless governing equations were solved using an implicit finite-difference method of Crank-Nicolson type. A parametric study was performed to illustrate the influence of emerging thermophysical parameters on the velocity, temperature and concentration profiles. The local and average Nusselt number, Sherwood number and Skin-friction are presented graphically. The results obtained were compared with previously published ones and found to be in excellent agreement. This study is applicable in transport of fires in porous media (forest fires), in the design of high temperature chemical processing systems and solar energy systems.

Keywords: Dissipation, radiation, Dufour, Soret, MHD, chemical reaction/heat generation

Introduction

Thermal radiation plays a major role in some industrial applications such as glass production and furnace design; and in space technology applications, such as cosmical flight aerodynamics rocket, propulsion systems, plasma physics and space craft reentry aerothermodynamics which operate at high temperature. The processes involving high temperatures, the radiative heat transfer in combination with conduction, convection and mass transfer, play a very important role in the design of pertinent equipments in the areas such as nuclear power plants, gas turbines and the various propulsion devices for aircraft, missiles, satellites and space vehicles.

Chemical reaction is a process that leads to transformation of one set of chemical substances to another. These chemical reactions are usually characterized by chemical changes at a given temperature and chemical concentration to yield one or more products which have properties different from the reactants. Chemical reactions are central to chemical engineering where they are used for synthesis of new compound from natural raw materials such as petroleum, mineral ores and thermite reaction to generate light and heat in pyrotechnics and welding.

Magneto-hydrodynamics (MHD) (Magneto fluid dynamics or hydromagnetics) is the study of dynamics of electrically conducting fluids. Examples of such fluid include plasma, liquid metal and salt water or electrolytes. The fundamental concept behind MHD is that magnetic field can induce currents in a moving conductive fluid, which in turn creates forces on the fluid and also changes the magnetic field itself.

Heat transfer is a process by which internal energy from one substance transfers to another, while mass transfer is the transport of a substance (mass) in liquid or gaseous media. Heat and mass transfer occur simultaneously in many processes such as drying evaporation of a wet body, energy transfer in a wet cooling tower, flow in a desert cooler, polymer production and food processing. The energy flux (rate of energy transfer per unit area) and mass flux (rate of mass flow per unit area) can either be generated by temperature gradients or composition gradients. The energy caused or generated by composition gradient is known as Dufour or diffusion-thermo effect while the flux created or generated by temperature gradients is known as Soret or thermal-diffusion effect. Thermal-diffusion effect is considered useful in isotope separation, and diffusion-thermo effect is useful in mixture of gases with very light molecular weight (Hydrogen-helium) and of medium molecular weight (Nitrogen air) Kafoussians and Williams (1995). Hence, it is of interest to combine Heat and Mass transfer with Chemical Reaction MHD, Heat Generation, Dufour and Soret effects because of their applications in many processes occuring both in nature and industries involving fluid flow.

In view of these applications, Chamkha (1997) investigated non-darcy fully developed mixed convection in a porous medium channel with heat generation/absorbtion and hydromagnetic effects. Loganatha *et al*. (2011) studied the effect of chemical reaction on an unsteady, two dimensional laminar flow of a Viscous incompressible viscosity and thermal conductivity.

Chamkha *et al*. (2001) studied the radiation effects on the free convection flow past a semi-infinite vertical plate with mass transfer. Muthucumaraswamy and Senthil (2004) investigated the heat and mass transfer effect on moving vertical plate in the presence of thermal radiation. Ramachandra *et al*. (2007) considered the radiation and mass transfer effects on two-dimensional flow past an impulsively started isothermal vertical plate.

The interaction of radiation with hydromagnetic flow has become industrially more prominent in processes where high temperature occur.

Chaudhary *et al*. (2006) studied the radiation effects with simultaneous thermal and mass diffusion in MHD mixed convection flow from a vertical surface with ohmic heating. Emad and Gamal (2005) investigated the thermal radiation effects on MHD flow past a semi-infinite vertical plate in the presence of mass diffusion. Ramachandra *et al*. (2006a) studied finite difference analysis of radiative free convection flow past an impulsively started vertical plate with variable heat and mass flux.

In astrophysical regimes, the presence of planetary debris, cosmic dust etc, create a suspended medium saturated with plasma fluids. As in other porous media problems such as geo-mechanics and insulation engineering, the convectional approach is to simulate the pressure drop across the porous regime using early linear model. Satapathy *et al*. (1998)

studied radiation and free convection flow through porous medium. With regard to thermal radiation heat transfer flows in porous media Raptis and Singh (1985) studied free convection flow past an impulsively started vertical plate in a Darcian porous medium. Abd El-Naby *et al*. (2004) presented a finite difference solution of radiation effects on MHD unsteady free convectional flow over a vertical porous plate.

In many situations there may be an appreciable temperature difference between the surface and ambient fluid. This necessitates the consideration of temperature dependent heat sources or sinks which may exert strong influence on the heat generation or absorption in moving fluids. This is important in view of several physical problems, such as fluids undergoing exothermic or endothermic chemical reactions. Representative studies dealing with these effects have been reported by Vajravelu and Hadijinicolaou (1993) and Chamkha (1997). Pop and Soundalgekar (1962) studied viscous dissipation effects on unsteady free convective flow past an infinite porous plate with variables sunction.

Ramachandra *et al*. (2006b) analysed the radiation effects on MHD free convection flow with mass transfer past a semi-infinite vertical plate in the presence of heat source/sink. Chamkah *et al*. (2003) considered the thermal radiation effects on MHD forced convection adjacent to a non-isothermal weldge in the presence of heat source or sink. Bala and Bhaskar (2010) studied radiation effects on MHD combined convection and mass transfer flow past a vertical porous plate embedded in a porous medium with heat generation.

In numerous chemical engineering processes, there exist chemical reaction between a foreign mass and the fluid in which the plate is moving. These processes take place in many industrial applications such as: polymer production, manufacturing of ceramics or glassware and food processing.

Muthucumaraswamy and Chandrakala (2006) studied radiative heat and mass transfer effects on moving isothermal vertical plate in the presence of chemical reaction. Afify (2004) investigated the effect of radiation on free convective flow and mass transfer past a vertical isothermal cone surface with chemical reaction in the presence of a transverse magnetic field. Suneetha and Bhaskar (2011) studied radiation and Darcy effects on unsteady MHD heat and mass transfer flow of chemically reacting fluid past an impulsively started vertical plate with heat generation.

However the interaction of dissipitation, radiation, Dufour, Soret with heat and mass transfer in a chemically reacting and electrically conducting fluid past an impulsively started vertical plate embedded in a non-Darcy porous medium in the presence of heat generation has received no attention, to the best of the authors' knowledge. Hence the present study is attempted. This study has significant applications in solar collection systems, fire dynamics in insulations, and also geothermal energy system. The volumetric heat generation term may exert a strong influence on the heat transfer and as a consequence also on the fluid flow.

Mathematical Formulation

The study under investigation concerns an unsteady two-dimentional hydromagnetic, laminar natural convection flow of a viscous, incompressible, dissipitating, radiating and chemically reacting fluid past an impulsively started vertical plate embedded in a porus medium in the presence of heat generation.

The fluid is assumed to be grey, absorbing-emitting but not-scattering.

The governing boundary-layer equations of the problem are formulated in a (*x**, *y**, *t**) coordinate system with appropriate boundary conditions. The *y**- axis is taken perpendicular to the plate at the leading edge while *x**- axis is chosen along the plate in the vertical upward direction. The origin of *x**- axis is taken to be at the leading edge of the plate. The gravitational acceleration \lq g\rq is acting downward. At time *t**=0, it is assumed that the plate and the fluid are at the same ambient temperature T_∞^* and the species concentration C_∞^* , when *t**>0, the temperature of the plate and the species concentration are maintained at T_w^* (such that $T_w^* > T_\infty^*$) and C_w^* (such that $C_w^* > C_\infty^*$).

At time *t**=0, the plate commences impulsive motion in the *x**-direction, with constant velocity u_0, and the plate temperature and concentration levels are instantaneously elevated and are maintained constantly thereafter. The corresponding configuration of the system is as shown in Fig. 1.

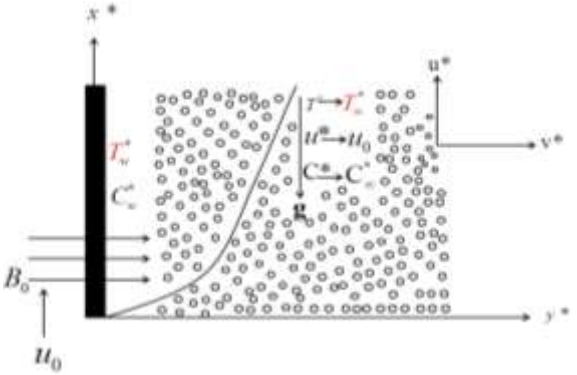

Fig. 1: Configuration of the system

The Rosseland diffusion approximation is used to analyze the radiative heat flux in the energy equation which is appropriate for non-scattering media. A parametric study was performed to illustrate the influence of the emerging thermophysical parameters on the velocity, temperature and concentration profiles. Also the local and average skin-friction, Nusselt number, Sherwood number, Soret number and Dufour number are presented graphically.

The fluid properties are assumed to be constant except for the body forces terms in the momentum equation which is approximated by Boussinesq relations. Thermal radiation is assumed to be present in the form of an uni-directional flux in the *y**-direction i.e. q_r is transverse to the vertical surface.

The Rosseland diffusion flux is used and defined following Modest (1993) as follows:

$$q_r = \frac{-4\sigma \partial T^{*4}}{3k' \partial y^*} \qquad (1)$$

Where σ is the Stefan-Boltzmann constant and k' is the mean absorption coefficient

As expressed by Rapits and Perdikis (2004), the quartic temperature function T^{*4} is expanded in Taylor series and neglecting higher order terms if the temperature differences within the flow are sufficiently small to obtain

$$T^{*4} \approx 4T_\infty^{*3} - 3T_\infty^{*4} \qquad (2)$$

Using (2) in (1) we have;

$$q_r = \frac{16\sigma}{3k'} T^{*3} \frac{\partial T^*}{\partial y^*} \qquad (3)$$

The governing equations: continuity, momentum, energy and species equations of the problem with Boussinesq approximation are given as follows:

Continuity: $\frac{\partial u^*}{\partial x^*} + \frac{\partial u^*}{\partial y^*} = 0$ (4)

Momentum:
$$\frac{\partial u^*}{\partial t^*}+u^*\frac{\partial u^*}{\partial x^*}+v^*\frac{\partial u^*}{\partial y^*}=\nu\frac{\partial^2 u^*}{\partial y^{*2}}+g_x\beta\left(T^*-T_\infty^*\right)+g_x\beta\left(C^*-C_\infty^*\right)-\frac{\sigma}{\rho}B_0^2u^*-\frac{\mu}{k}u^*-\frac{b}{k}u^{*2} \quad (5)$$

Energy:
$$\frac{\partial T^*}{\partial t^*}+u^*\frac{\partial T^*}{\partial x^*}+v^*\frac{\partial T^*}{\partial y^*}=\alpha\frac{\partial^2 T^*}{\partial y^{*2}}+\frac{\nu}{C_p}\left[\frac{\partial u^*}{\partial y^*}\right]^2+\frac{Q_0}{\rho C_p}\left(T^*-T_\infty^*\right)+D_mk_T\frac{\partial^2 C^*}{\partial x^{*2}}+\frac{16\sigma T_\infty^{*3}}{3k'\rho C_p}\cdot\frac{\partial^2 T^*}{\partial y^{*2}} \quad (6)$$

and Species:
$$\frac{\partial C^*}{\partial t^*}+u^*\frac{\partial C^*}{\partial x^*}+v^*\frac{\partial C^*}{\partial y^*}=D\left[\frac{\partial^2 u^*}{\partial y^{*2}}\right]-k_1C^*+D_mk_T\frac{\partial^2 T^*}{\partial y^{*2}} \quad (7)$$

Where u^*, v^* are velocity components in x^*,y^* directions respectively. t^* - the time, g - the acceleration due to gravity, β - the volumetric coefficient of thermal expansion, β^* - the volumetric coefficient of expansion with concentration, T^* - the temperature of the fluid in the boundary layer, C^* - the species concentration in the boundary layer, T_w^* - the wall temperature, T_∞^* - the free stream temperature far away from the plate, C_w^* - the concentration at the plate, C_∞^* - the free stream concentration in fluid far away from the plate, k' - the permeability of porous medium, B_0 - Magnetic induction, ν - the kinematic viscosity of the grey fluid, α - the thermal diffusivity, ρ - the density of fluid, C_p - the specific heat at constant pressure, q_r - the radiation heat flux, Q_0 - the heat generation/absorption constant, D - the species diffusion coefficient, σ - fluid electric conductivity, and k_1 - the chemical reaction parameter.

The corresponding initial and boundary conditions for the study are given as follows:

$$\begin{aligned}
&t^*\le 0,\ u^*=0,\ v^*=0,\ T^*=T_\infty^*,\ C^*=C_\infty^*\\
&t^*>0,\ u^*=u_0^*,\ v^*=0,\ T^*=T_w^*,\ C^*=C_w^*,\quad at\ y^*=0\\
&\qquad u^*=0,\qquad T^*=T_\infty^*,\ C^*=C_\infty^*,\quad at\ x^*=0\\
&\qquad u^*\to 0,\qquad T^*\to T_\infty^*,\ C^*\to C_\infty^*,\quad at\ y^*\to 0
\end{aligned} \quad (8)$$

The following dimensionless variables and parameters were then introduced,

$$\left.\begin{aligned}
&X=\frac{x^*u_0}{\nu},\ Y=\frac{y^*u_0}{\nu},\ U=\frac{u^*}{u_0},\ V=\frac{v^*}{u_0},\ E_c=\frac{u_0}{C_p\left(T_w^*-T_\infty^*\right)}\\
&t=\frac{t^*u_0^2}{\nu},\ T=\frac{T^*-T_\infty^*}{T_w^*-T_\infty^*},\ C=\frac{C^*-C_\infty^*}{C_w^*-C_\infty^*},\ \mathrm{Re}=\frac{u_0L}{\nu}\\
&Q=\frac{Q_0\nu}{\rho C_pu_0^2},\ \mathrm{P}_r=\frac{\nu}{a},\ S_c=\frac{\nu}{D},\ D_a=\frac{K}{L^2},\ F_s=\frac{b}{L},\ N=\frac{k'k}{4\sigma T_\infty^{*3}}\\
&M=\frac{\sigma B_0^2\nu}{u_0^2},\ G_r=\frac{g\beta\nu\left(T_w^*-T_\infty^*\right)}{u_0^3},\ G_m=\frac{g\beta^*\nu\left(C_w^*-C_\infty^*\right)}{u_0^3}\\
&K=\frac{K_1\nu}{u_0^2},\ S_r=\frac{D_mK_T\left(T_w^*-T_\infty^*\right)}{\rho C_p\nu\left(C_w^*-C_\infty^*\right)},\ D_u=\frac{D_mK_T\left(C_w^*-C_\infty^*\right)}{\rho C_p\nu\left(T_w^*-T_\infty^*\right)}
\end{aligned}\right\} \quad (9)$$

Using the dimensionless variables in equation (9) the governing equations (4), (5), (6) and (7) are reduced to the following non-dimensional forms

$$\frac{\partial U}{\partial X}+\frac{\partial V}{\partial Y}=0 \tag{10}$$

$$\frac{\partial U}{\partial t}+U\frac{\partial U}{\partial X}+V\frac{\partial U}{\partial Y}=\frac{\partial^2 U}{\partial Y^2}+G_r T+G_m C-MU-\frac{U}{D_a\,\mathrm{Re}^2}-\frac{F_s U^2}{D_a\,\mathrm{Re}} \tag{11}$$

$$\frac{\partial T}{\partial t}+U\frac{\partial T}{\partial X}+V\frac{\partial T}{\partial Y}=E_c\left[\frac{\partial U}{\partial Y}\right]^2+\frac{1}{P_r}\left[1+\frac{4}{3N}\right]\frac{\partial^2 T}{\partial Y^2}+QT+D_u\frac{\partial^2 C}{\partial X^2} \tag{12}$$

$$\frac{\partial C}{\partial t}+U\frac{\partial C}{\partial X}+V\frac{\partial C}{\partial Y}=\frac{1}{S_c}\frac{\partial^2 C}{\partial Y^2}+S_r\frac{\partial^2 T}{\partial Y^2}-KC \tag{13}$$

The corresponding dimensionless initial and boundary conditions are:

$$\begin{aligned} &t\le 0, \quad U=0,\ V=0,\ T=0,\ C=0 \\ &t>0, \quad U=1,\ V=0,\ T=1,\ C=1, \quad at\ Y=0 \\ &\qquad\ U=0,\ T=0,\ C=0, \quad at\ X=0 \\ &\qquad\ U\to 0,\ T\to 0,\ C\to 0, \quad at\ Y\to\infty \end{aligned} \tag{14}$$

Where X and Y are dimensionless coordinates, U and V are dimensionless velocities, t is dimensionless time, T is dimensionless temperature function, C is the dimensionless concentration function, μ is the conduction radiation heat transfer parameter, P_r is the Prandtl number, S_c is the Schimdt number, *Re* is the Reynold number, D_a is the Darcy number, F_s is the Forchheimer (non-Darcy) inertia number, G_r is the thermal Grashof number, G_m is the species Grashof number, M is the magnetic field parameter, E_c is the Eckert number, N is the radiation parameter, Q is the dimensionless heat generation/absorption coefficient, K is the chemical reaction parameter, S_r is the Soret number (constant), and D_u is the Dufour number (constant).

For the type of flow under consideration, the local as well as the average values of skin-friction, Nusselt number and Sherwood number are important, and the dimensionless form of these are defined as follows:

Local skin-frictions

$$\tau=-\left(\frac{\partial U}{\partial Y}\right)_{Y=0} \tag{15}$$

Average skin-frictions

$$\overline{\tau}=-\int_0^1\left(\frac{\partial U}{\partial Y}\right)_{Y=0}dX \tag{16}$$

Local Nusselt number

$$Nu_x=-X\left(\frac{\partial T}{\partial Y}\right)_{Y=0} \tag{17}$$

Average Nusselt number

$$\overline{Nu}=-\int_0^1\left(\frac{\partial T}{\partial Y}\right)_{Y=0}dX \tag{18}$$

Local Sherwood number

$$Sh_x=-X\left(\frac{\partial C}{\partial Y}\right)_{Y=0} \tag{19}$$

Average Sherwood number

$$\overline{Sh}=-\int_0^1\left(\frac{\partial C}{\partial Y}\right)_{Y=0}dX \tag{20}$$

Method of solution

The non-linear coupled differential equations (10), (11), (12) and (13) with the boundary conditions (14) by a finite difference scheme of the Crank-Nicolson type. The partial differential equations were converted to difference equations which resulted to a tri-diagonal matrix system. Prasad *et al*. (2007) used Crank-Nicolson scheme to analyze Transient convective heat and mass transfer with thermal radiation effects along vertical impulsively started plate. Seth and Sarka (2015) also used Crank-Nicolson Scheme to analyse the hydro magnetic natural convection flow with induced magnetic field and *n*th order chemical reaction of a heat absorbing fluid past an impulsively moving vertical plate with ramped temperature. Also, Siraiah *et al*. (2010) used Crank-Nicolson scheme to analyze the radiation effects on MHD free convection flow over a vertical plate with heat and mass flux. Ime *et al*. (2014) used Crank-Nicolson scheme to analyze convective heat and mass transfer flow over a vertical plate with *n*th order chemical reaction in a porous medium. This scheme has been extensively developed in recent years and remains one of the best reliable schemes for solving partial differential equations. All the authors mentioned above did not consider the scheme for the solution of dissipation, radiation, Dufour and Soret effects on heat and mass transfer of chemically reacting fluid with heat generation and that has motivated us to embark on this work.

In this study, the coordinate (X,Y,t) of the mesh points of the solution are defined by $X=i\Delta X$, $Y=j\Delta Y$ and $t=k\Delta t$ where i, j, and k are positive

integers and the value of U at these mesh points are denoted by $U(i\Delta X\,,\, j\Delta Y\,, k\Delta t) = U_{i,j}^{k}$.

The region of integration in this study is considered to be a rectangle with sides $X_{\max} = 1$ and $Y_{\max}$ corresponding to $Y = \infty$ which lie very well outside the momentum and thermal boundary layers. Following Suneetha and Bhaskar (2011), X varies from 0 to 1, Y varies from 0 to $Y_{\max} = 14$ and X=1 corresponds to the height of the plate. The subscript i implies the grid point along X-direction, j along Y-direction, k along t-direction. We divided X and Y-directions into M and N grid spacing points respectively. The mesh sizes are $\Delta X = 0.05,\ \Delta Y = 0.25$ and $\Delta t = 0.01$.

The finite difference equations corresponding to the transient coupled non-linear partial differential equations (10), (11), (12) and (13) are given as follows:

$$\frac{\left[U_{i,j}^{k+1} - U_{i-1,j}^{k+1} + U_{i,j}^{k} - U_{i-1,j}^{k} + U_{i,j-1}^{k+1} - U_{i-1,j-1}^{k+1} + U_{i,j-1}^{k} - U_{i-1,j-1}^{k}\right]}{4(\Delta X)} + \frac{\left[V_{i,j}^{k+1} - V_{i,j-1}^{k+1} + V_{i,j}^{k} - V_{i,j-1}^{k}\right]}{2(\Delta Y)} = 0 \tag{21}$$

$$\frac{U_{i,j}^{k+1} - U_{i,j}^{k}}{\Delta t} + \frac{U_{i,j}^{k}}{2(\Delta X)}\left[U_{i,j}^{k+1} - U_{i-1,j}^{k+1} + U_{i,j}^{k} - U_{i-1,j}^{k}\right] + \frac{V_{i,j}^{k}}{4(\Delta Y)}\left[U_{i,j+1}^{k+1} - U_{i,j-1}^{k+1} + U_{i,j+1}^{k} - U_{i,j-1}^{k}\right]$$
$$= \frac{G_r}{2}\left[T_{i,j}^{k+1} + T_{i,j}^{k}\right] + \frac{G_m}{2}\left[C_{i,j}^{k+1} + C_{i,j}^{k}\right] + \frac{\left[U_{i,j-1}^{k+1} - 2U_{i,j}^{k+1} + U_{i,j+1}^{k+1} + U_{i,j+1}^{k} - 2U_{i,j}^{k} - U_{i,j-1}^{k}\right]}{2(\Delta Y)^2} \tag{22}$$
$$- \frac{1}{2D_a\,\mathrm{Re}^2}\left[U_{i,j}^{k+1} + U_{i,j}^{k}\right] + \frac{F_s}{2D_a\,\mathrm{Re}}U_{i,j}^{k}\left[U_{i,j}^{k+1} + U_{i,j}^{k}\right] - \frac{M}{2}\left[U_{i,j}^{k+1} + U_{i,j}^{k}\right]$$

$$\frac{1}{\Delta t}\left[T_{i,j}^{k+1} - T_{i,j}^{k}\right] + \frac{U_{i,j}^{k}}{2(\Delta X)}\left[T_{i,j}^{k+1} - T_{i-1,j}^{k+1} + T_{i,j}^{k} - T_{i-1,j}^{k}\right] + \frac{V_{i,j}^{k}}{4\Delta Y}\left[T_{i,j+1}^{k+1} - T_{i,j-1}^{k+1} + T_{i,j-1}^{k} + T_{i,j+1}^{k} - T_{i,j-1}^{k}\right]$$
$$= E_c\left[\frac{U_{i,j+1}^{k} - U_{i,j}^{k}}{2(\Delta Y)}\right]^2 + \frac{1}{P_r}\left[1 + \frac{4}{3N}\right]\frac{\left[T_{i,j-1}^{k+1} - 2T_{i,j}^{k+1} + T_{i,j-1}^{k+1} + T_{i,j+1}^{k} - 2T_{i,j}^{k} + T_{i,j-1}^{k}\right]}{2(\Delta Y)^2} \tag{23}$$
$$+ D_u\frac{\left[C_{i+1,j}^{k+1} - 2C_{i,j}^{k+1} + C_{i-1,j}^{k+1} + C_{i+1,j}^{k} - 2C_{i,j}^{k} + C_{i-1,j}^{k}\right]}{2(\Delta X)^2}$$

$$\left[\frac{C_{i,j}^{k+1} - C_{i,j}^{k}}{\Delta t}\right] + \frac{U_{i,j}^{k}}{2(\Delta X)}\left[C_{i,j}^{k+1} - C_{i-1,j}^{k+1} + C_{i,j}^{k} - C_{i-1,j}^{k}\right] + \frac{V_{i,j}^{k}}{4(\Delta Y)}\left[C_{i,j+1}^{k+1} - C_{i,j-1}^{k+1} + C_{i,j+1}^{k} - C_{i,j-1}^{k}\right]$$
$$= \frac{1}{S_c}\frac{\left[C_{i+1,j}^{k+1} - 2C_{i,j}^{k+1} + C_{i,j-1}^{k+1} + C_{i,j-1}^{k} - 2C_{i,j}^{k} + C_{i,j+1}^{k}\right]}{2(\Delta Y)^2} \tag{24}$$
$$+ \frac{S_r}{2(\Delta Y)^2}\left[T_{i,j+1}^{k+1} - 2T_{i,j}^{k+1} + T_{i,j-1}^{k+1} + T_{i,j+1}^{k} - 2T_{i,j}^{k} + T_{i,j-1}^{k}\right] - \frac{K}{2}\left[C_{i,j}^{k+1} + C_{i,j}^{k}\right]$$

The finite difference equations (21), (22), (23) and (24) are now written in a tri-diagonal matrix system as follows

$$-V_{i,j-1}^{k+1} + V_{i,j}^{k+1} = F_1 \tag{25}$$
$$-A_2U_{i,j-1}^{k+1} + B_2U_{i,j}^{k+1} + D_2U_{i,j+1}^{k+1} = F_2 \tag{26}$$
$$-A_3T_{i,j-1}^{k+1} + B_3T_{i,j}^{k+1} + D_3T_{i,j+1}^{k+1} = F_3 \tag{27}$$
$$-A_4C_{i,j-1}^{k+1} + B_4C_{i,j}^{k+1} + D_4C_{i,j+1}^{k+1} = F_4 \tag{28}$$

Where,

$$F_1 = E_1\left(U_{i,j}^{k+1} - U_{i-1,j}^{k+1} + U_{i,j}^{k} - U_{i-1,j}^{k} + U_{i,j-1}^{k+1} - U_{i-1,j-1}^{k+1} + U_{i,j-1}^{k} - U_{i-1,j-1}^{k}\right) + V_{i,j-1}^{k} - V_{i,j}^{k} \tag{29}$$

$$\begin{aligned} &A_2 = -E_3 + E_6,\ B_2 = 1 + E_2 + 2E_6 + E_7 + E_8 + E_9,\ D_2 = \left(E_3 - E_6\right), \\ &F_2 = \left(E_3 + E_6\right)U_{i,j-1}^{k} + \left(1 - E_2 - 2E_6 - E_7 - E_8 - E_9\right)U_{i,j}^{k} - \left(E_3 - E_6\right)U_{i,j+1}^{k} \\ &\quad + E_4\left(T_{i,j}^{k+1} + T_{i,j}^{k}\right) + E_5\left(C_{i,j}^{k+1} + C_{i,j}^{k}\right) + 2E_2U_{i-1,j}^{k+1} + 2E_2U_{i-1,j}^{k} \end{aligned} \tag{30}$$

$$\begin{aligned} &A_3 = \left(E_3 + E_{10}\right),\ B_3 = \left(1 + E_2 + 2E_{10} + E_{13}\right),\ D_3 = \left(E_3 + E_{10}\right), \\ &F_3 = \left(E_3 + E_{10}\right)T_{i,j-1}^{k} + \left(1 - E_2 - 2E_{10} + E_{13}\right)T_{i,j}^{k} - \left(E_3 - E_{10}\right)T_{i,j+1}^{k} + E_2T_{i-1,j}^{k+1} \\ &\quad + E_{11}\left(U_{i,j+1}^{k} - U_{i,j}^{k}\right)^2 + E_{12}\left(C_{i+1,j}^{k+1} + 2C_{i,j}^{k+1} + C_{i-1,j}^{k+1} + C_{i+1,j}^{k} - 2C_{i,j}^{k} + C_{i-1,j}^{k}\right) \end{aligned} \tag{31}$$

$$\begin{aligned} &A_4 = \left(E_3 + E_{14}\right),\ B_4 = \left(1 + E_2 + 2E_{14} + E_{16}\right),\ D_4 = \left(E_3 + E_{14}\right), \\ &F_4 = \left(E_3 + E_{14}\right)C_{i,j-1}^{k} + \left(1 - E_2 - 2E_{14} + E_{16}\right)C_{i,j}^{k} - \left(E_3 - E_4\right)C_{i,j+1}^{k} + E_2C_{i-1,j}^{k} \\ &\quad + E_2C_{i-1,j}^{k+1} + E_{15}\left(T_{i,j+1}^{k+1} + 2T_{i,j}^{k+1} + C_{i,j-1}^{k+1} + T_{i,j+1}^{k} - 2T_{i,j}^{k} + T_{i,j-1}^{k}\right) \end{aligned} \tag{32}$$

$$\left.\begin{aligned} &E_1 = -\frac{\Delta Y}{2\Delta X},\ E_2 = \frac{\Delta t}{2\Delta X}U_{i,j}^{k},\ E_3 = \frac{\Delta t}{4\Delta Y}V_{i,j}^{k},\ E_4 = \frac{\Delta tG_r}{2},\ E_5 = \frac{\Delta tG_m}{2}, \\ &E_6 = \frac{\Delta t}{2\left(\Delta Y\right)^2},\ E_7 = \frac{\Delta t}{2D_a\,\mathrm{R}_e^2},\ E_8 = \frac{\Delta tF_s}{2D_aR_e}U_{i,j}^{k},\ E_9 = \frac{\Delta tM}{2}, \\ &E_{10} = \frac{1}{P_r}\left[1 + \frac{4}{3N}\right]\frac{\Delta t}{2\left(\Delta Y\right)^2},\ E_{11} = \frac{\Delta tE_c}{4\left(\Delta Y\right)^2},\ E_{12} = \frac{\Delta tD_u}{2\left(\Delta X\right)^2},\ \text{and}\ E_{13} = \frac{\Delta tQ}{2} \end{aligned}\right\} \tag{33}$$

In the computations as discussed in Muthucumarasuuamy and Senthil (2004), the coefficient $U_{i,j}^{k}$ and $V_{i,j}^{k}$ appearing in the difference equations are treated as constants in any one time step. The values of *C*, *T*, *U* and *V* are known at all grid point at *t* =0 from the initial conditions. The values of *C*, *T*, *U* and *V* at time level (*k+1*) were calculate using the known values at previous time level (*k*). The finite difference equations forms a tridiagonal systems of equations at every internal nodal point on a particular *i*-level which are solved with the aid of Matlab package using Thomas Algorithm as discussed in Carnaha *et al*. (1969) and Suneetha and Bhaskar (2011).

Using (28), the value of *C* on a given *i*-level at time level was known at every nodal point and this was used to calculate the value of *C* at time (*k+1*) level. Also the value of *T* at time (*k+1*) level was calculated in the same way *C* was calculated using equation (27). The results obtained from *C* and *T* at time (*k+1*) level are used in equation (26) to calculate *U* at time (*k+1*) level. Hence the values of *C*, *T* and *U* are known on a particular *i*-levels. In this way, the values of *C*, *T* and *U* are known at all grid point. The values of *V* are also calculated at every nodal point explicitly using equation (25) on a particular *i*-level at $(k+1)^{th}$ time level.

The local truncation error is of $O\left(\Delta t^2 + \Delta Y^2 + \Delta X\right)$ and it tends to zero as each of Δt , ΔY and ΔX tends to zero. This indicates that the system is compatible since Crank-Nicolson scheme is always unconditionally stable. Compatibility and stability ensure the convergence of the scheme.

Discussion of Results

Computations are carried out to study the effects of fluid parameters such as magnetic field (*M*), thermal radiation parameter (*N*), Schmidt number (S_c) Viscous dissipation function (E_c), thermal Grashof number (G_r), modified Grashof number (G_m), permiability parameter (D_a), Prandt number (P_r), Soret number (S_r) and Dufour number (D_u) on the dimensionless, velocity, temperature and concentration profiles. All graphs correspond to the following default values except stated otherwise on the graph P_r = 0.71, S_c = 0.62, N = 3.0. M = 1.0. G_r = 2.0, G_m = 2.0, R_e = 1.0, E_c = 0.001, F_s = 0.1, D_a = 0.3, n = 1.5.

In order to validate the present numerical scheme we compared the present solutions with that of Sunetha and Bhaskar Reddy (2011) who have employed Crank-Nicolson Scheme for the same flow field in the absence of Dufour, Soret, dissipitation and radiation (Fig. 2). It is found that there is a good agreement.

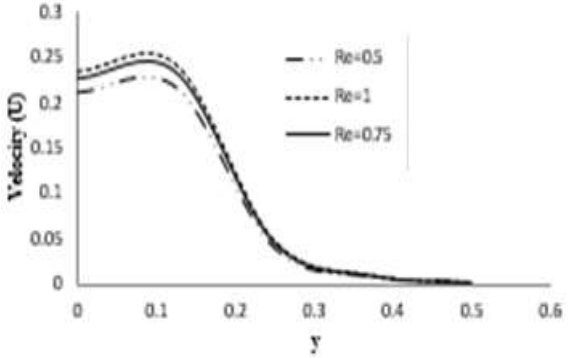

Fig. 2: Effects of *Re* on velocity profile

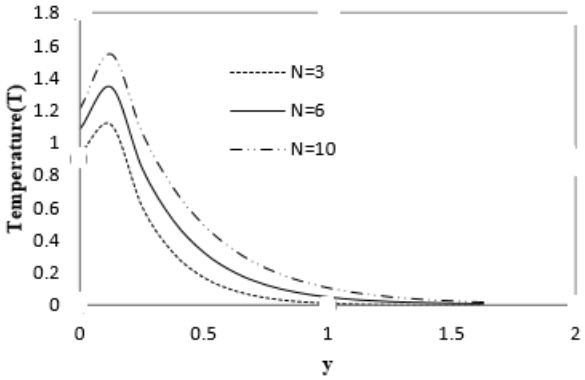

Fig. 3: Effects of N on temperature profile

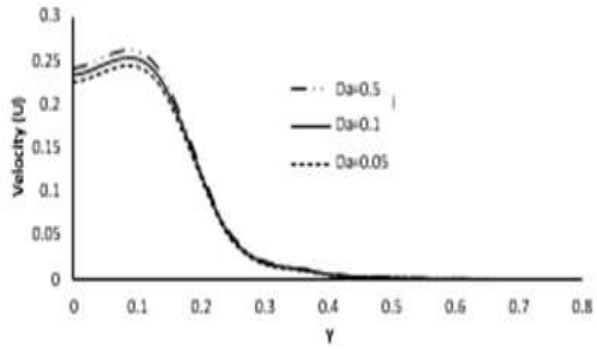

Fig. 4: Effects of D_a on velocity profile

Figures 3 and 4 show the effects of radiation (*N*) and Darcy number (D_a). A rise in *N* causes an increase in the temperature values at the wall (*y*=0) across the boundary layer to the free stream. Hence, greater value of *N* corresponds to high radiation flux and the highest temperature is observed for *N*=10 in Fig. 3. Thermal radiation thereby reduces the rate of energy transport to the fluid. In Fig. 4, as Darcy number increases a rise in velocity profile is experienced. This rise in velocity profile means that conduction heat transfer is more prevalence than convection heat transfer.

Figure 5 illustrates the effect of the magnetic field (*M*) on the dimensionless velocity profile. An increase in the magnetic field causes a reduction in the velocity profile. The presence of magnetic field on an electrically conducting fluid results in increasing the Lorentz force which opposes and retards motion of fluid. Fig. 6 shows the influence of *Sc* on the concentration profile. With large value of *Sc*, the fluid experience lower diffusion properties that is concentration boundary layer becomes thinner than the velocity boundary layer thickness. A rise in *Sc* through 0.6 to 3.6 and 3.6 to 6.6 produce a decrease in concentration.

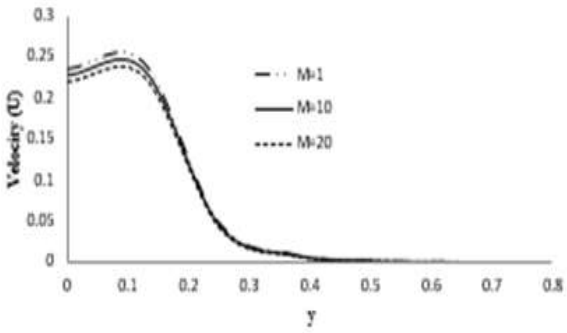

Fig. 5: Effects of M on velocity profile

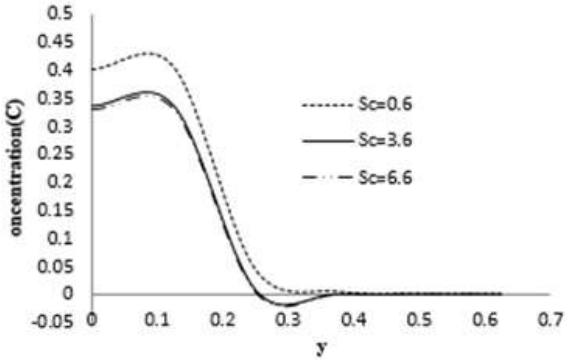

Fig. 6: Effects of Sc on concentration profile

Figure 7 shows the effect of P_r on the dimensionless temperature profile. *Pr* is the ratio of momentum diffusivity to thermal diffusivity i.e., it controls the thickness of thermal boundary layer and the rate of heat transfer. The numerical results show that as Prandtl number increases, we experience a decrease in the thermal boundary layer thickness and in general this lowers the average temperature. This is because smaller value of P_r increases the thermal conductivity of the fluid which indicates that heat is able to diffuse away from the heated surface more rapidly than with higher value of P_r. Temperature across the boundary layer normal to the wall reduces to zero faster for higher P_r values.

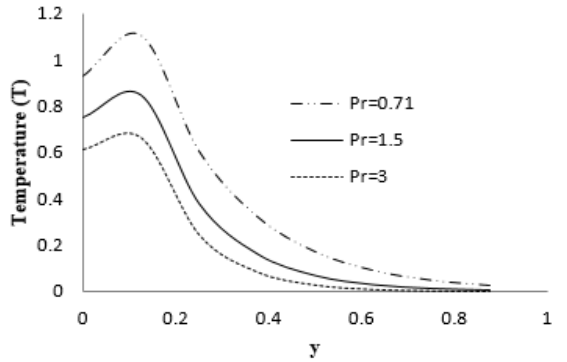

Fig. 7: Effects of Pr on temperature profile

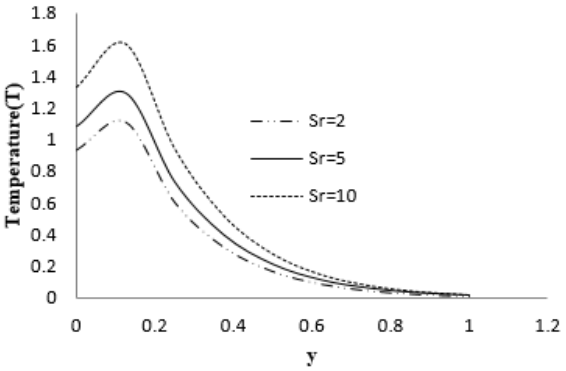

Fig. 8: Effects of S_r on temperature profile

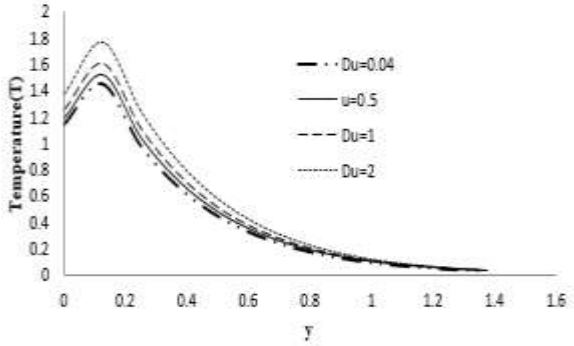

Fig. 18: Effects of D_u on temperature profile

Figure 8 illustrates the effect of Soret (S_r) on temperature profile. As S_r increases we experience greater increase in the temperature profile. The temperature decreases asymptotically to zero from the highest value at the wall to zero in the free stream. Fig. 9 shows the effect of Dufour (D_u) on dimensionless temperature profile and an increase in Dufour brings about increase in the temperature.

Figure 10 depicts the effect of Soret (S_r) on the dimensionless concentration profile. As S_r increases we experience great increase in concentration profile. The concentration decreases asymptotically to zero from the highest value at the wall to zero in the free stream.

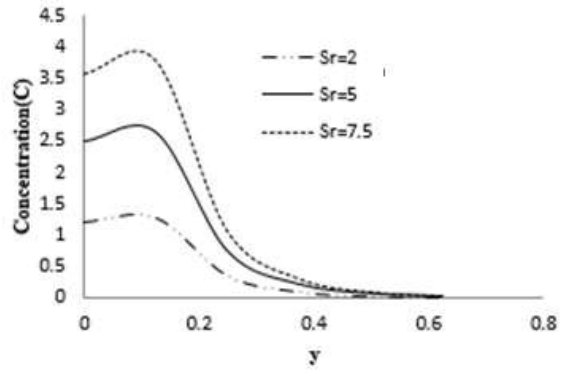

Fig. 10: Effects of S_r on concentration profile

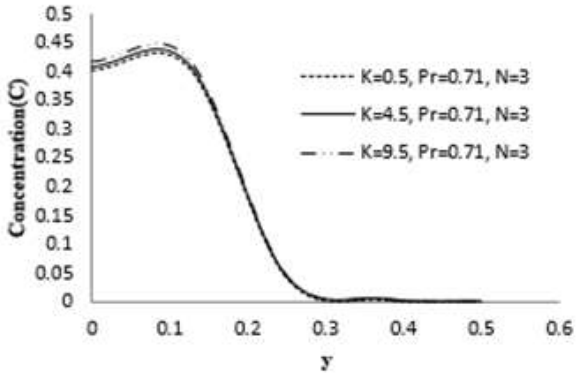

Fig. 11: Effects of K on concentration profile

Figure 11 shows transient concentration profile for different values of *K*. It is observed that as *K* increases, concentration profile decreases which show that an increase in *K* leads to a fall in concentration.

Conclusion

This study deals with the effects of dissipation, radiation, Dufour, Soret, heat and mass transfer flow in a gray absorbing-emitting fluid-saturated non-darcy porous medium adjacent to an impulsively started vertical surface with heat generation and chemical reaction. The Rosseland diffusion flux model has been used to simulate the radiative heat flux. The family of governing partial differential equations is solved by an implicit difference scheme of Crank-Nicolson type. A parametric study is performed to illustrate graphically the influence of the thermophysical parameters on the dimensionless velocity, temperature and concentration profiles. It has been observed that:

- Increase in the thermal radiation parameter N caused a rise in temperature values from the highest values close to the wall (y=0) across the boundary layer to the free stream. Thus, greater value of N corresponds to high radiation flux and the highest temperature are observed for N=10.
- As D_a increases in Thermal radiation parameter a rise in velocity profile is experienced.
- The conduction heat transfer is more prevalence than convection heat transfer.
- An increase in the magnetic field (M) causes reduction in the velocity profile.
- With large value of S_c the fluid experiences lower diffusion properties i.e., concentration boundary layer is thinner than the velocity boundary layer thickness. A rise in S_c produces a decrease in concentration.
- As P_r increases the fluid experiences a decrease in the thermal boundary layer thickness.
- As S_r increases great increase in the temperature profile is experienced.
- Also an increase in S_r leads to an increase in concentration profile. The concentration decreases asymptotically to zero from the highest value at the wall to zero in the free stream.
- An increase in Dufour brings about increase in the temperature.
- As K (chemical reaction parameter) increases concentration profile decreases.

Conflict of Interest

Authors declare that there is no conflict of interest related to this study.

References

Abd El-Naby MA, Elsayed ME & Nader YA 2004. Finite difference solution of radiation effects on the MHD free convection flow over a vertical porous plate. *Appl. Math. Comp.*, 151: 327-346.

Afify AA 2004. Effects of radiation on free convecture flow and mass transfer past a vertical isothermal cone surface with chemical reaction in the presence of a transverse magnetic field. *Canadian J. Phys.*, 82: 447-458.

Bala Anki RP & Bhaskar RN 2010. Radiation effects on MHD combined convection and mass transfer flow past a vertical porous plate embedded in a porous medium with heat generation. *Int. J. Appl. Math and Mech.*, 6(18): 33-49.

Chamkha AJ 1997. Non-Darcy fully developed mixed convection in a porous medium channel with heat generation/absorbtion and hydromagnetic effects. *Numer. Heat Transfer*, 32: 853-875.

Chamkha AJ, Takhar HS & Soundalgekar VM 2001. Radiation effects on free convection flow past a semi-infinite vertical plate with mass transfer. *Chem. Engr. J.*, 84: 335-342.

Chaudhary RC, Bhupendra KS & Abhay KJ 2006. Radiation effect ith Simultaneous thermal and mass diffusion in MHD mixed convection flow from a vertical Surface with ohmic heating. *Romanian J. Phy.*, 51(7-8): 715-727.

Kafoussian NG & Williams EW 1995. Thermal diffusion-thermo effects on mixed free forced convective and mass transfer boundary layer flow with temperature dependent viscosity. *Int. J. Engr. Sci.*, 33: 1369-1384.

Loganatha P, Iranian D & Ganesan P 2011. Effect of chemical reaction on unsteady free convective and mass transfer flow past a vertical plate with variable viscosity and thermal conductivity. *European J. Scientific Res.*, 59(31): 403-416.

Modest MF 1993. Radiation Heat Transfer. MacGraw-Hill, New York.

Muthucumaraswamy R & Chandrakala P 2006. Radiative heat and mass transfer effects on moving isothermal vertical plate in the presence of chemical reaction. *Int. J. Appl. Mech. and Engr.*, 11: 639-646.

Muthucumaraswamy R & Sentthil G 2004. Heat and mass transfer effects on moving particle plate in the presence of thermal radiation. *Theoretical Applied Mechanics*, 31: 35-46.

Pop I & Soundalgekar VM 1962. Viscous dissipation effects on unsteady free convective flow past an infinite vertical porous plate with variable suction. *Int. J. Heat Mass Transfer*, 17: 852-92.

Prasad RV, Reddy BN & Muthueumaraswamy R 2007. Radiation and mass transfer effect on two-dimensional flow past an impulsively started infinite vertical plate. *Int. J. Thermal Sci*., 46(12): 1251-1258.

Ramachandra PV & Bhaskar RN 2007. Radiation and mass transfer effects on an unsteady MHD free convection flow past a heated vertical plate in a porous medium with viscous dissipation. *Theoretical. Applied Mechanics*, 34(2): 135-160.

Ramachandra PV, Bhaskar RN & Muthucumaraswamy R 2006a. Finite difference analysis analysis of radiative free convection flow past an impulsively started vertical plate with variable heat and mass flux. *J. Appl. Theo. Mech.*, 3: 31-63.

Ramachandra PV, Bhaskar RN & Muthucumaraswamy R 2006b. Finite difference analysis of radiation effects on MHD free Convection flow with mass transfer past a Semi-infinite vertical plate in the presence of heat source/sink. *Int. Rev. Pure and Appl. Math.*, 2(2): 141-160.

Raptis A & Singh AK 1985. Free convection flow past an impulsively started vertical plate in a porous medium by finite difference method. *Astrophysics and Space Science*, 112: 259- 265.

Satapathy S, Bedford A, Bless S & Raptis A 1998. Radiation and free convection flow through a porous medium. *Int. Comm. Heat Mass Transfer*, 25: 289 -297.

Seth GS & Sarka S 2015. Hydromagnetic natural convection flow with induced magnetic field and n^{th} order chemical reaction of a heat absorbing fluid past an impulsively moving vertical plate with ramped temperature. *Bulgarian Chemical Communications*, 47(1): 66-79.

Siraiah M, Nagarajan AS & Sreehari RP 2010. Radiation effects on MHD free convection flow over a vertical plate with heat and mass flux. *Int. Comm. Heat Mass Transfer*, 25: 289 -297.

Suneetha S & Bhaskar RN 2011. Radiation and Darcy effects on unsteady MHD heat and mass transfer flow of a chemically reacting fluid past an impulsively started vertical plate with heat generation. *J Appl. Math. and Mech.*, 7(7): 1-19.

Vajravelu K & Hadjinicolaou A 1993. Heat transfer in a viscous fluid over a Streching sheet with viscous dissipation and internal heat generation. *Int. Comm. Heat Mass Transfer*, 20: 417-430.